Article

J. Biol. Regul. Homeost. Agents. 2024; 38(6): 4879–4893
https://doi.org/10.23812/j.biol.regul.homeost.agents.20243806.390

Novel N6-Methyladenosine-Associated lncRNA Model for Predicting Biochemical Recurrence in Patients with Prostate Cancer

Yufan Wu[1,2,†], Qizhong Lu[1,2,†], Xi Zhang[2], Linya Yao[2], Xueming Zeng[2], Qiwei Yu[2,*], Weiguo Chen[1,*]

[1]Department of Urology, The First Affiliated Hospital of Soochow University, 215000 Suzhou, Jiangsu, China
[2]Department of Urology, Kunshan Hospital of Traditional Chinese Medicine, 215300 Kunshan, Jiangsu, China
*Correspondence: yqweifly@163.com (Qiwei Yu); chenweiguo1971@suda.edu.cn (Weiguo Chen)
[†]These authors contributed equally.
Submitted: 13 February 2023 Revised: 15 March 2023 Accepted: 8 June 2023 Published: 1 June 2024

Background: Prostate cancer (PC) is a solid tumour that is highly prevalent worldwide, ranking as the second most common tumour in humans. The N6-methyladenosine modification of ribonucleic acid (RNA) (m6A) is the most prevalent epigenetic internal modification of both non-coding RNAs (ncRNAs) and messenger RNAs (mRNAs). This study aimed to investigate the link between m6A-related long non-coding RNAs (lncRNAs) and PC to provide a new solution for treating this disease.

Methods: This study used a Pearson's correlation analysis to identify m6A-related lncRNAs. The expression and function of AC020907.4, one of the four selected m6A-related lncRNAs, were verified through experimental validation in PC tissue samples and cell lines. In addition, univariate Cox regression was employed to screen these m6A-related lncRNAs for PC. In the validation and entire groups, a least absolute shrinkage and selection operator (LASSO) Cox regression analysis was used to establish and validate the prognostic model for biochemical recurrence (BCR), and small interfering RNA (siRNA) was used to knockdown AC020907.4. Real-time quantitative polymerase chain reaction assay was used to detect the mRNA expression level. A cell counting kit-8 assay was used to detected cell viability.

Results: In total, this study identified 204 m6A-related lncRNAs and found that 64 of the 204 were linked with BCR in patients diagnosed with PC. The LASSO Cox regression was employed to establish a BCR model containing four lncRNAs (AC020907.4, AC022364.1, AC099850.3 and AP001505.1). Kaplan–Meier curves confirmed the different outcomes in the low-risk and high-risk groups. The effectiveness of the model was evaluated using receiver operating characteristic and concordance index curves. The independence of the model for the prognosis prediction was analysed using univariate and multivariate Cox regression analyses. The knockdown of AC020907.4 reduced the cell viability of PC cells.

Conclusions: This study constructed and validated an m6A-related lncRNA model for BCR prediction in patients with PC, providing new insights for research related to m6A and the clinical treatment of PC.

Keywords: prostate cancer; N6-methyladenosine-associated lncRNA; m6A; prognostic model; biochemical recurrence

Introduction

Prostate cancer (PC) is a solid tumour that is highly prevalent worldwide, ranking as the second most common tumour in humans. In 2021, it was the fifth leading cause of cancer deaths in men [1,2]. Currently, if patients develop localised PC, the optimal results are achieved through radical prostatectomy (RP). However, after RP, approximately 27%–53% of patients develop prostate-specific biochemical recurrence (BCR) because of the inherent heterogenicity of PC [3,4]. According to the guidelines provided by the European Association of Urology, BCR can be identified if the prostate-specific antigen value, the most commonly recognised diagnostic biomarker of PC, rises to 0.2 ng/mL with an upward trend at two consecutive follow-up appointments after RP [5]. It is well known that BCR does not equal clinical recurrence, which can be confirmed through imaging examinations. Although not all patients progress to BCR after RP, BCR remains a key risk factor for the total mortality of PC [6]. Distinguishing patients who have a high risk of BCR from those with a low risk is crucial so that rescue therapy can be administered to high-risk patients promptly. Although a number of prognostic models have been developed and used for the prediction of the overall survival (OS) of patients with PC after treatment [7], a model is urgently needed for use in clinics as an early predictor of BCR.

The N6-methyladenosine modification of ribonucleic acid (RNA) (m6A) is a major epigenetic modification of different types of RNAs, including non-coding RNAs (ncR-

Journal of
BIOLOGICAL REGULATORS
and Homeostatic Agents

NAs) and messenger RNAs (mRNAs) [8]. The methylation of RNA has been demonstrated to regulate its stability, maturation, cellular export and decay [9–11]. The m6A methylation is a dynamically reversible RNA modification. This modification is regulated by three m6A modulators: writers (methyltransferases that put m6A on RNAs), readers (proteins that can recognise the m6A site in RNAs) and erasers (demethylases that remove m6A from RNAs) [12,13].

Multiple studies have shown that m6A patterns of mRNA (abundance and location) are vital for assessing the progression and pathogenesis of different types of cancers [8,14,15]. For example, research suggested that methyltransferase 3 (METTL3) promotes the translation of mRNAs that are related to the pathogenesis of human lung cancer, including the Hippo pathway effector tafazzin and epidermal growth factor receptor [14]. Methylation regulators have been associated with the clinicopathological features of PC, and prognostic models constructed using genes involved in m6A methylation have a high predictive value for recurrence after RP [15].

Long non-coding RNAs (lncRNAs) contain <200 nucleotides with no standard open reading frame, and they do not encode any proteins [16]. The abnormal expression of lncRNAs is linked with a variety of cancers and has key functions in regulating the cell cycle and its differentiation; it also impacts the apoptosis, proliferation, invasion and metastasis of different cancer cells [17,18]. Some studies have shown that lncRNAs can be utilised as biomarkers for predicting the progression and diagnosis of PC [19,20]. In addition, some reports have noted that m6A can occur extensively on a variety of lncRNAs to change their stability, resulting in abnormal transcription and gene expression [21–23]. Ni *et al*. [24] found that the m6A reader protein, YTH N6-methyladenosine RNA binding protein (YTHDF) 3, can increase the degradation of lncRNA GAS5 by affecting its m6A modification, thereby facilitating the yes-associated protein pathway in colorectal cancer (CRC). Thus, targeting the m6A of GAS5 may be a novel treatment for CRC [24]. Lang *et al*. [25] reported that m6A promotes PC bone metastasis and tumour growth; however, the detailed pathogenesis mechanism of how m6A-modified lncRNAs affect PC has not been fully investigated.

In this study, through a study of The Cancer Genome Atlas (TCGA) [26] datasets (n = 499) and Chinese Prostate Cancer Genome and Epigenome Atlas (CPGEA) [27,28] datasets (n = 208), 204 m6A-related lncRNAs were identified in patients with PC. Subsequently, in the training group, 64 m6A-related lncRNAs were predicted to be related to PC. This study also established a model of m6A-related lncRNAs for the prediction of the likelihood that a patient with PC may progress to BCR. This research may assist with the improved prediction of prognosis in patients with PC, thus providing earlier interventional therapies in high-risk patients that may progress to BCR.

Materials and Methods

Expression of mRNA and Clinical Data

The mRNA expression datasets from the PC tissue samples and adjacent normal tissue specimens were downloaded from TCGA (https://portal.gdc.cancer.gov/) and CPGEA (https://ngdc.cncb.ac.cn/bioproject/browse/PRJCA001124). As of 29 October 2021, the datasets contained 707 PC tissue samples and 260 samples from adjacent non-tumour tissue. The corresponding information from clinical data (e.g., identity, survival time and state, tumour (T)–node (N)–metastasis stage, age, ethnicity, BCR state, BCR time and Gleason score) was downloaded from the University of California at Santa Cruz Xena website (https://xenabrowser.net/datapages/?dataset). The local research ethics committee indicated no additional ethical clearance was required because the initial research that generated these data was conducted in accordance with TCGA and CPGEA standards.

Identification of the Differentially Expressed m6A Modulators

In total, 22 m6A modulators were identified from previous research, including m6A writers (methyltransferase *(METTL)3/14/16*, *RBM15*, *RBM15B*, *VIRMA*, *WTAP* and *ZC3H13*), readers (*HNRNPC*, *IGF2BP2/3*, *RBMX*, *YTHDC1/2*, *YTHDF1/2/3*, etc.) and erasers (alkB homolog 5 (*ALKBH5*) and alpha-ketoglutarate-dependent dioxygenase (*FTO*)) [23]. The edgeR software (Version 100.0.1185.29, Bioconductor, Redmond, WA, USA) package [29] was used to identify the differentially expressed m6A modulators ($p < 0.05$). A Venn diagram was drawn based on the differentially expressed m6A modulators from TCGA and CPGEA data.

Identification of m6A-Related lncRNAs

The m6A-related lncRNAs in PC were identified using Pearson's correlation analysis. In this study, m6A-related lncRNAs were defined as lncRNAs that have correlation coefficients > 0.5 and a p-value < 0.05. The results were visualised through a Sankey diagram using the ggplot2 function in R [30].

Establishment of an m6A-Related lncRNA Model

The m6A-related lncRNA model was established using a least absolute shrinkage and selection operator (LASSO) Cox regression analysis [31], as in previous studies [32]. The stratified randomisation method was used to separate the patients into training and validation groups (5:5). The biomarkers were identified in the training group, and the validation group was used to evaluate the identified regression. The LASSO Cox regression analysis was utilised to analyse the expression of m6A-related lncRNAs and determine the prognostic model. Finally, receiver operating characteristic (ROC) curves [33], Kaplan–Meier sur-

vival estimates and concordance index (C-index) curves [34] were used to evaluate the power of the model in predicting the prognosis of patients with PC.

Patients and Clinical Specimens

Ten PC specimens and their paired healthy tissue were collected from the patients undergoing laparoscopic RP at the urology department of Kunshan Hospital of Traditional Chinese Medicine between June 2018 and December 2020. All tissue samples were stored in liquid nitrogen. The specimen and clinical pathological data collection were approved by the Institutional Research Ethics Committee of Kunshan Hospital of Traditional Chinese Medicine, and written informed consent was obtained. The ethical approval number for this study was KZY2020-09.

Cell Culture

Two human PC cell lines (C4-2B and DU145) and human normal prostate epithelial cell line RWPE-1 cells were purchased from the Shanghai Chinese Academy of Sciences cell bank (Shanghai, China). The PC cell lines were grown in Dulbecco's Modified Eagle Medium (11995040, Gibco, Grand Island, NY, USA), which was supplemented with 10% foetal bovine serum (10270-106, Gibco, Grand Island, NY, USA) and 1% penicillin–streptomycin. The RWPE-1 cells were cultured in keratinocyte serum-free medium, which contained human recombinant epidermal growth factor (PHG0311, Thermo Fisher Scientific, Waltham, MA, USA) (5 ng/mL) and bovine pituitary extract (02-104, Sigma-Aldrich, Saint Louis, MO, USA) (0.05 mg/mL). All cell lines have passed mycoplasma detection and STR identification. All cells were free of mycoplasma contamination and no additional cell contamination.

RNA Extraction and Real-Time Quantitative Polymerase Chain Reaction Assays

The total RNA of the PC specimens and paired healthy tissue were extracted using Ezol Reagent (B002-v001, GenePharma, Shanghai, China). The target complementary deoxyribonucleic acid was synthesised through reverse transcription (RT) using random primers and the GoScript RT system (A5001, Promega, Madison, WI, USA). A real-time quantitative polymerase chain reaction (qRT-PCR) was performed using GoTaq qPCR Master Mix (A6001, Promega, Madison, WI, USA) and qRT-PCR Plus System (Stratagene, La Jolla, CA, USA). Data processing was performed using the $2^{-\Delta\Delta Ct}$ method. The results are presented as mean ± standard deviation (n = 3 replicates). A two-tailed Student's *t*-test or one-way analysis of variance (ANOVA) was used for statistical analysis.

The sequences of the *METTL3*, *AC020907.4* and glyceraldehyde-3-phosphate dehydrogenase (*GAPDH*) primers were as follows:

METTL3 forward:
5′-TTGTCTCCAACCTTCCGTAGT-3′;
METTL3 reverse:
5′-CCAGATCAGAGAGGTGGTGTAG-3′;
AC020907.4 forward:
5′-GGCAGAGGTCGCACCACTG-3′;
AC020907.4 reverse:
5′-CCCACAGCCAGCCTTTGAGAA-3′;
GAPDH forward:
5′-ATCACCATCTTCCAGGAGCG-3′;
GAPDH reverse:
5′-CAAATGAGCCCCAGCCTTC-3′.

Cell Transfection

Small interfering RNA (siRNA) targeting AC020907.4 (siRNA-1 and siRNA-2) and the negative control (NC) were purchased from GenePharma (Shanghai, China). The *AC020907.4* siRNA-1 was 5′-CCAGCUGCAGGUAAGUGCUCAGUCU-3′, and the *AC020907.4* siRNA-2 was 5′-CAGCUGCAGGUAAGUGCUCAGUCUA-3′. The siNC was 5′-AAUAAACUUUGCUUGUGUUGGGUGG-3′. Lipofectamine 2000 (Invitrogen, Carlsbad, CA, USA) was applied according to the instructions.

Cell Counting Kit-8 Assay

Cell proliferation rates were measured using a cell counting kit-8 (CCK-8; GW770, Dojindo, Tokyo, Japan) assay. The transfected C4-2B and DU145 cell lines (5×10^3 cells/well) were seeded in a 96-well plate. After 0, 24, 48 and 72 h of culture, 10 µL of CCK-8 solution was added, after which the cells were incubated for 2 h at 37 °C. The absorbance was measured in a microplate reader (Multiskan SkyHigh, Thermo Fisher Scientific, Waltham, MA, USA) at 450 nm.

m6A RNA Methylation Quantification

Total RNA isolation and two rounds of PloyA+ mRNA selection were performed to measure the global change of the m6A modification level. The change in global m6A levels in the mRNA was measured using an EpiQuik m6A RNA Methylation Quantification Kit (EpiGentek, cat. P-9005, New York, NY, USA) following the manufacturer's protocol.

Univariate and Multivariate Cox Regression Analyses

Univariate and multivariate Cox regression analyses were used to evaluate the model's independence from the available clinical data (e.g., age, Gleason score, T/N stage and ethnicity) to predict the prognosis. Statistical Product and Service Solutions (SPSS) 19.0 software (IBM, Chicago, IL, USA) was employed to calculate the two-tailed hazard ratios and 95% confidence intervals.

Journal of
BIOLOGICAL REGULATORS
and Homeostatic Agents

Functional Enrichment Analysis and Immunohistochemistry Analysis

The Gene Ontology (GO) annotations of the mRNAs that were differentially produced in the low-risk and high-risk groups were conducted using the ClusterProfiler function in R [35]. The immunohistochemistry figures of the m6A modulators were downloaded from the Human Protein Atlas Database (https://www.proteinatlas.org/) [36].

Statistical Analysis

The SPSS 19.0 software was used for statistical analyses. A two-tailed Student's *t*-test was performed for the comparison between two groups. One-way ANOVA was performed for comparisons between three or more groups based on one factor. A two-way ANOVA was performed for comparisons between three or more groups based on two factors. Univariate and multivariate Cox regression analyses were used to evaluate the model's independence from the available clinical data, and p values < 0.05 were considered statistically significant.

Results

Expression of m6A Modulators in Patients with PC

The analytical procedure is presented in the flowchart in Fig. 1. Data from TCGA and CPGEA included 707 PC tissue samples and 260 samples of adjacent non-tumour tissue, along with the clinical information. First, in the cancer and healthy tissue, 22 differentially expressed m6A modulators were identified (Fig. 2a,b). The number of differentially expressed ($p < 0.05$) m6A modulators in TCGA and CPGEA data was 18 and 17, respectively. Second, the m6A modulators with the same expression pattern in both TCGA and CPGEA data were identified using the Venn diagram shown in Fig. 2c. In total, 14 m6A modulators were used for further study. In addition, some of the differentially expressed m6A modulators were validated at protein level (data extracted from the Human Protein Atlas Database), as shown in **Supplementary Fig. 1a**. The link between the m6A modulator expression and Gleason score is shown in **Supplementary Fig. 1b**.

Recognition of m6A-Related lncRNAs

The m6A-related lncRNAs in TCGA data were found using Pearson's correlation analysis. In total, 204 lncRNAs were identified as m6A-related lncRNAs. Fig. 3a shows the potential relationship between the m6A modulators and lncRNAs using a Sankey diagram. To determine the prognostic models of these 204 lncRNAs, univariate Cox regressions for BCR were conducted, and 64 lncRNAs ($p < 0.05$) were identified as the m6A-related lncRNAs for prognostic prediction in patients with PC. A forest plot is shown in Fig. 3b.

Novel Model of m6A-Related lncRNA Established Using LASSO Regression in the Training Group

The LASSO method was employed for the construction of a novel and accurate prognostic model to simplify and normalise the m6A-related lncRNA model. The stratified randomisation method was used to separate patients equally into validation and training groups (5:5). The formula below was used to calculate the risk score in the m6A-related lncRNA model in the training group:

$$Risk\ score = \Sigma\ (Expi \times Coefi).$$

In the formula, for the specific lncRNA, *Expi* represents the expression level, and *Coefi* represents the estimated regression coefficient analysed using multivariate Cox regression. Fig. 4a displays the estimated coefficients analysed using the LASSO model, where the dotted line indicates the coefficient in the training group that is defined by cross-validation. In Fig. 4b, a generalised cross-validation plot of the expressions of the lncRNAs (training group) is visualised. The tuning parameter (the partial likelihood deviance against log [Lambda]) was also plotted. The most suitable Lambda occurred when five variables were shown in the model. Finally, the multivariate Cox regression analysis constructed a significant BCR-associated lncRNA model containing four lncRNAs: AC020907.4, AC022364.1, AC099850.3 and AP001505.1. The expression of the selected lncRNAs and association between the m6A modulators and these lncRNAs is plotted in Fig. 4c. In addition, the coefficients for AC020907.4, AC022364.1, AC099850.3 and AP001505.1 were 1.49, –1.13, 0.67 and 0.42, respectively.

m6A-Related lncRNA AC020907.4 Was Upregulated in PC Cells, and the Knockdown of AC020907.4 Can Inhibit PC Proliferation in Vitro

Since lncRNA AC020907.4 possessed the highest coefficient among the four selected lncRNAs, we decided to validate the expression of AC020907.4 in the PC tissue samples and cell lines. As shown in Fig. 4c, AC020907.4 is closely related to METTL3, which is widely regarded as an m6A writer in current studies. Thus, we conducted qRT-PCR to quantify METTL3 and AC020907.4 expression in PC tissue samples and cell lines. The METTL3 and AC020907.4 expression was upregulated in both the PC tissue samples and cell lines compared with healthy tissue (Fig. 5a,b,e,f). In addition, m6A levels in the PC tissue samples were higher than those in the paired healthy tissue (Fig. 5c). The expression of AC020907.4 was also positively correlated with m6A levels in the PC specimens (Fig. 5d). As shown in Fig. 5g,h, both siRNA-1 and siRNA-2 significantly reduced the expression of AC020907.4 in DU145 and C4-2B. Furthermore, the proliferation ability of DU145 and C4-2B was significantly reduced in both the siRNA-1 and siRNA-2 groups (Fig. 5i,j).

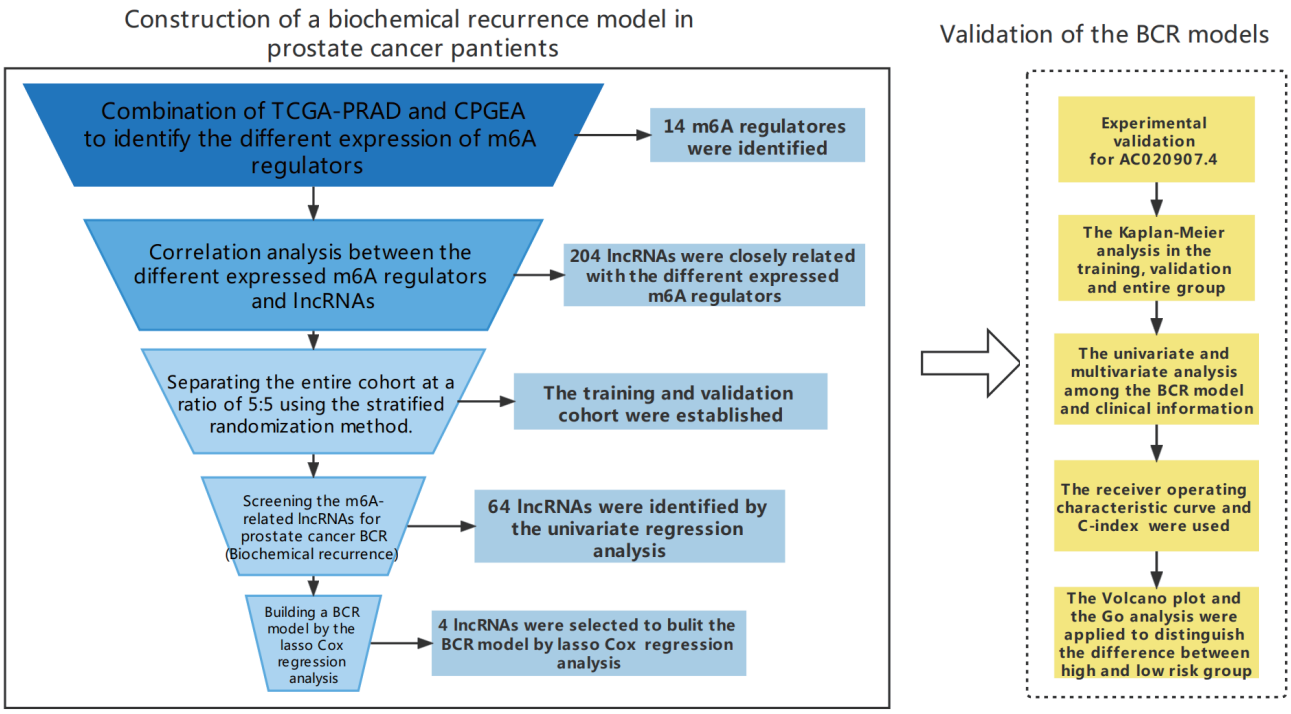

Fig. 1. Workflow to identify an m6A-related long non-coding RNA (lncRNA) model. Abbreviations: TCGA, The Cancer Genome Atlas; CPGEA, Chinese Prostate Cancer Genome and Epigenome Atlas; LASSO, least absolute shrinkage and selection operator; C-index, concordance index; BCR, biochemical recurrence; m6A, N6-methyladenosine modification of ribonucleic acid (RNA).

Effectiveness of the m6A-Related lncRNA Model for Predicting BCR Validated Using the Validation Group and Entire Group

Apart from the experimental validation of one selected lncRNA, the ability of the model to validate the prognostic power in different patients was evaluated. We applied the model to obtain the risk scores in the validation and entire groups. The optimal cutoff score was calculated using the Survminer function in R, and this value was employed to separate patients into low-risk and high-risk groups. As we expected, the validation and entire groups shared similar results with the training group; high-risk patients seemed to have a higher BCR frequency than those that were low-risk (Fig. 6). The Kaplan–Meier curves revealed the BCR frequency in the low-risk and high-risk patients in the different groups (Fig. 6a–c). The risk scores, distribution of patients and lncRNA expression in the different groups are displayed in Fig. 6d–l.

Independence from Other Clinical Information and Effectiveness of the Prognostic Model Validated through Multiple Approaches

To the best of our knowledge, the Gleason score and T/N stage are usually used to predict the prognosis of patients with PC. Therefore, univariate and multivariate Cox regression analyses were used to evaluate the independence of the model in predicting the prognosis of patients with PC. A significant difference ($p < 0.05$) was observed in the univariate Cox regression analysis when patients were grouped by the Gleason score, T/N stage and other predictors of the risk score. However, the age and ethnicity of patients did not correlate with BCR ($p > 0.05$) (Fig. 7a).

Subsequently, all factors were included in a multivariate Cox regression analysis (Fig. 7b). The results indicated that the 'risk score' variable was validated as independent for the prediction of a BCR prognosis ($p < 0.05$). The area under the curve (AUC) of the ROC curve was also employed to evaluate the prognostic ability of different predictors in Fig. 7c. The AUC of the risk score (0.764) was greater than those of other parameters containing clinical information. The time-dependent ROC curve in Fig. 7d indicated a model with improved performance and relatively high stability (these usually show a greater time-dependent AUC). The AUC values of the models were 0.764, 0.713 and 0.713 for 1-year, 3-year and 5-year BCR, respectively. The C-index curve also demonstrated that the risk score of the model had the highest C-index, indicating that the prognostic model was effective (Fig. 7e).

Journal of
BIOLOGICAL REGULATORS
and Homeostatic Agents

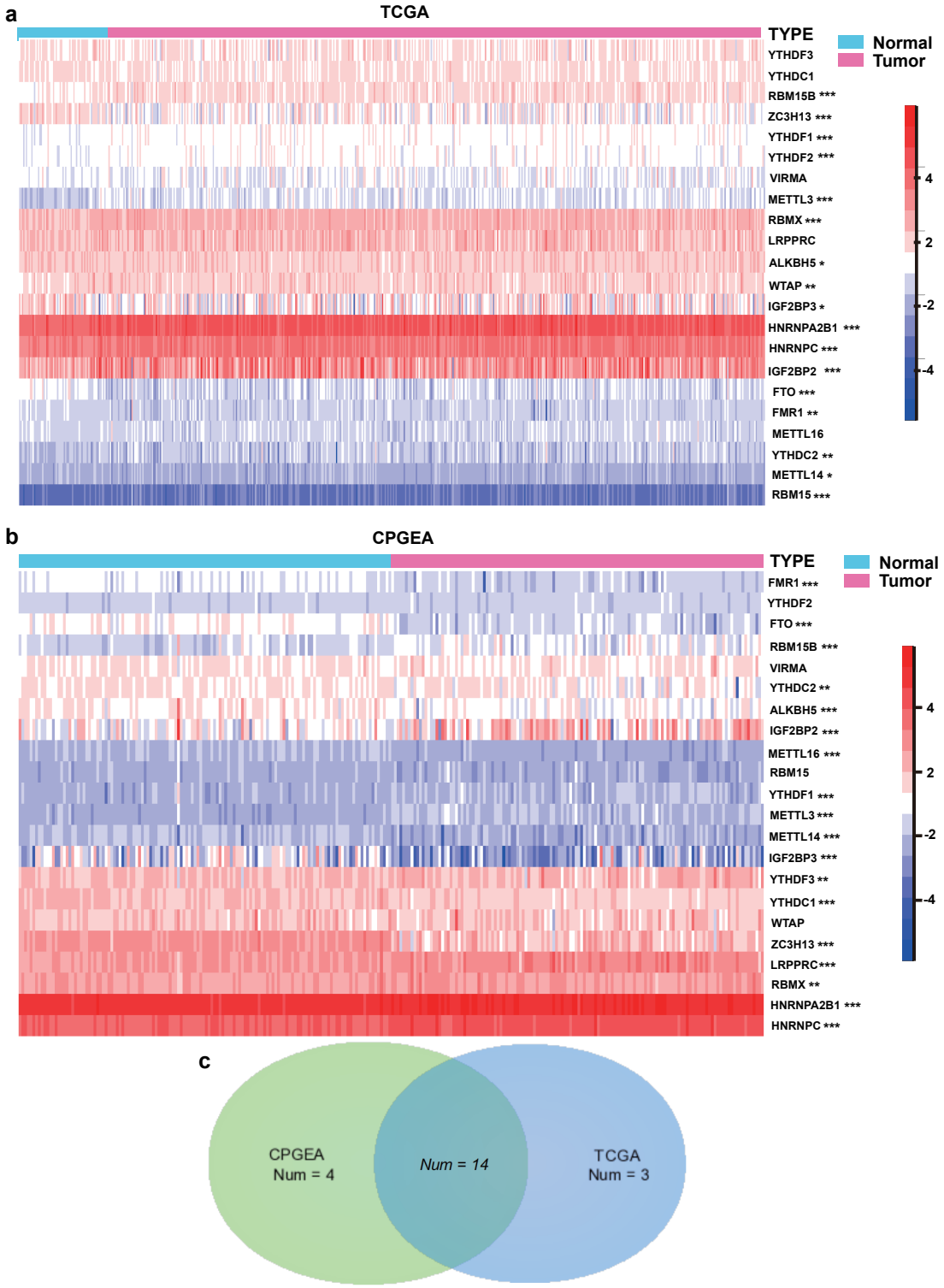

Fig. 2. Abnormal expression of m6A modulators in patients with prostate cancer (PC) at messenger RNA level. (a) Expression of 22 m6A modulators using data from patients with PC in The Cancer Genome Atlas (TCGA). (b) Expression of the 22 m6A modulators in patients with PC in the Chinese Prostate Cancer Genome and Epigenome Atlas (CPGEA). (c) Venn diagram of identified m6A modulators in TCGA and CPGEA. *: $p < 0.05$; **: $p < 0.01$; ***: $p < 0.001$. YTHDF, YTH N6-methyladenosine RNA binding protein; METTL, methyltransferase; ALKBH5, alkB homolog 5; FTO, alpha-ketoglutarate-dependent dioxygenase.

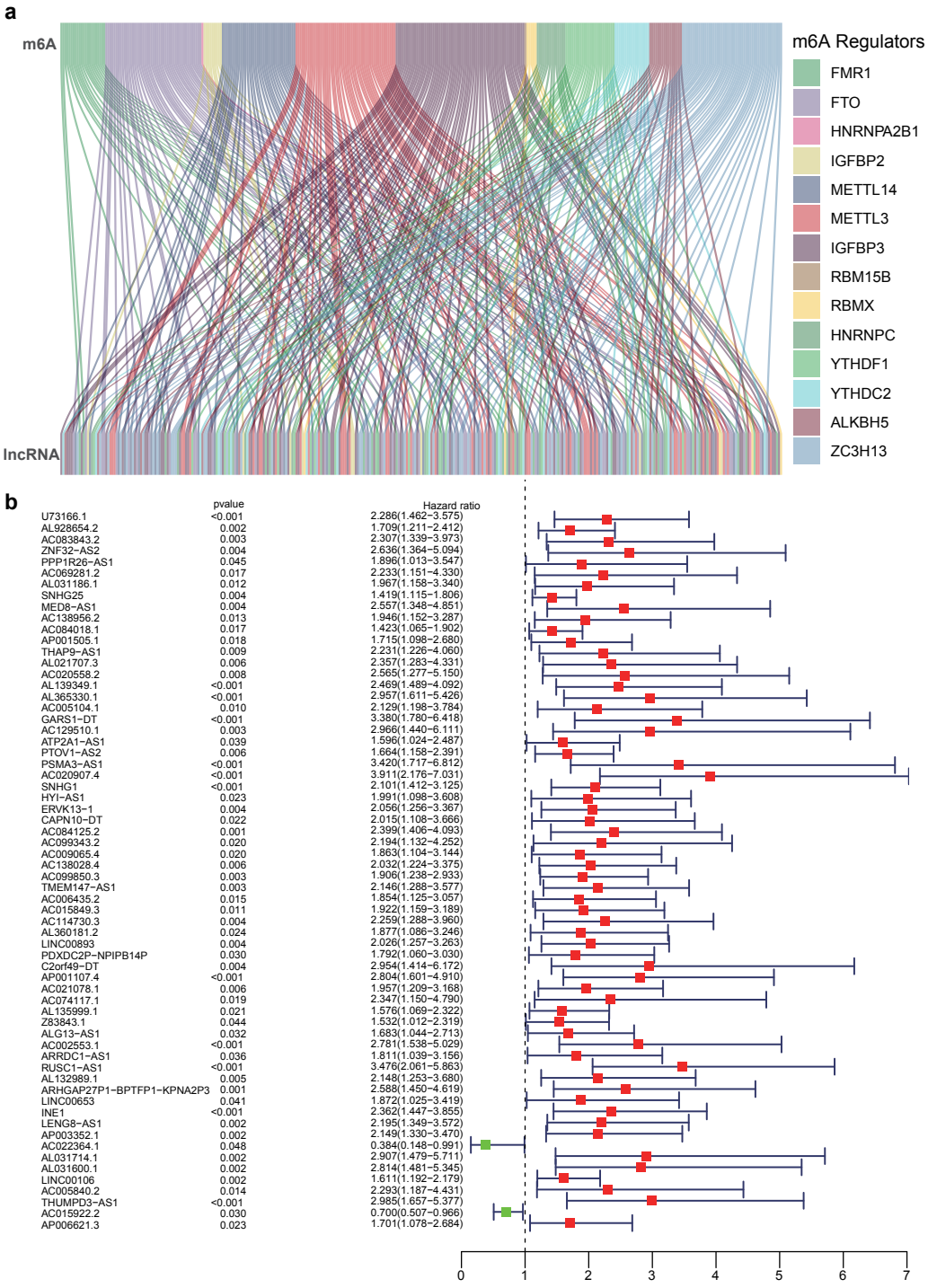

Fig. 3. Prognostic m6Arelated long non-coding RNA (lncRNA) identification in patients with prostate cancer. (a) Relationship between lncRNAs and m6A modulators using a Sankey diagram. (b) Univariate Cox regressions for biochemical recurrence using a forest plot.

m6A-Related lncRNA Model to Identify High-Risk Patients in the T3–4 Group

Because of the model's effective sensitivity, specificity and stability (time-dependent) for predicting BCR in patients with PC, we combined the risk score with the pathological features described previously to improve the model's prediction power using a Kaplan–Meier curve across the entire group. Fig. 8a,b indicates that the risk score can identify the high-risk patients with a Gleason score of ≤ 7 and >7. In Fig. 8c,d, the risk score can identify the high-risk patients in both the N0 and N1 groups. In

Journal of
BIOLOGICAL REGULATORS
and Homeostatic Agents

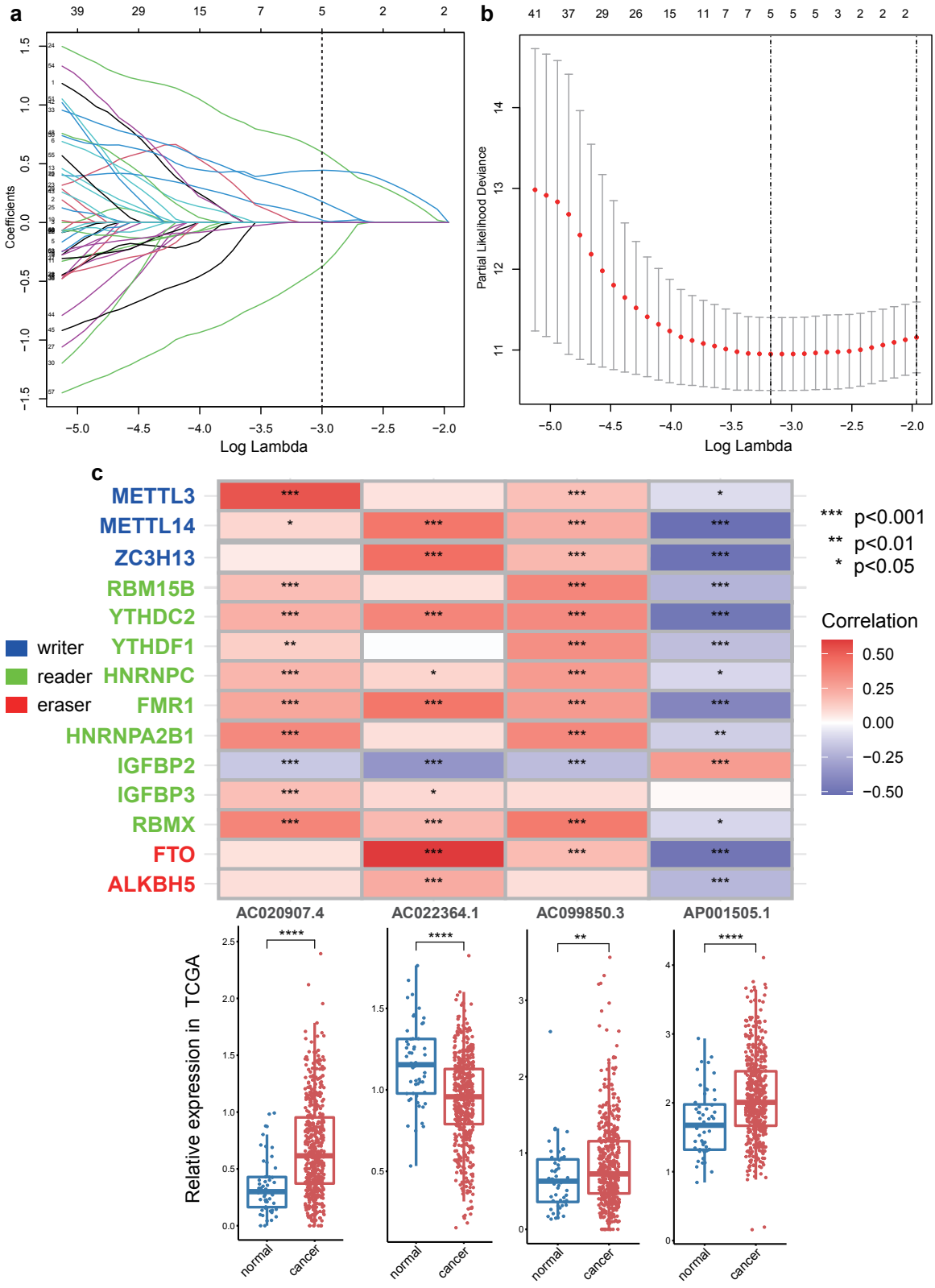

Fig. 4. Establishment of the m6A-related long non-coding RNA (lncRNA) model. (a) Least absolute shrinkage and selection operator coefficient values of the expression of five lncRNAs. The dotted lines indicate tenfold cross-validation. (b) Tenfold cross-validation for choosing the tuning parameters in the model. (c) Heatmap indicating the links between the m6A modulators and selected lncRNAs; the dotted plot shows the expression of the selected lncRNAs. *: $p < 0.05$; **: $p < 0.01$; ***: $p < 0.001$; ****: $p < 0.0001$.

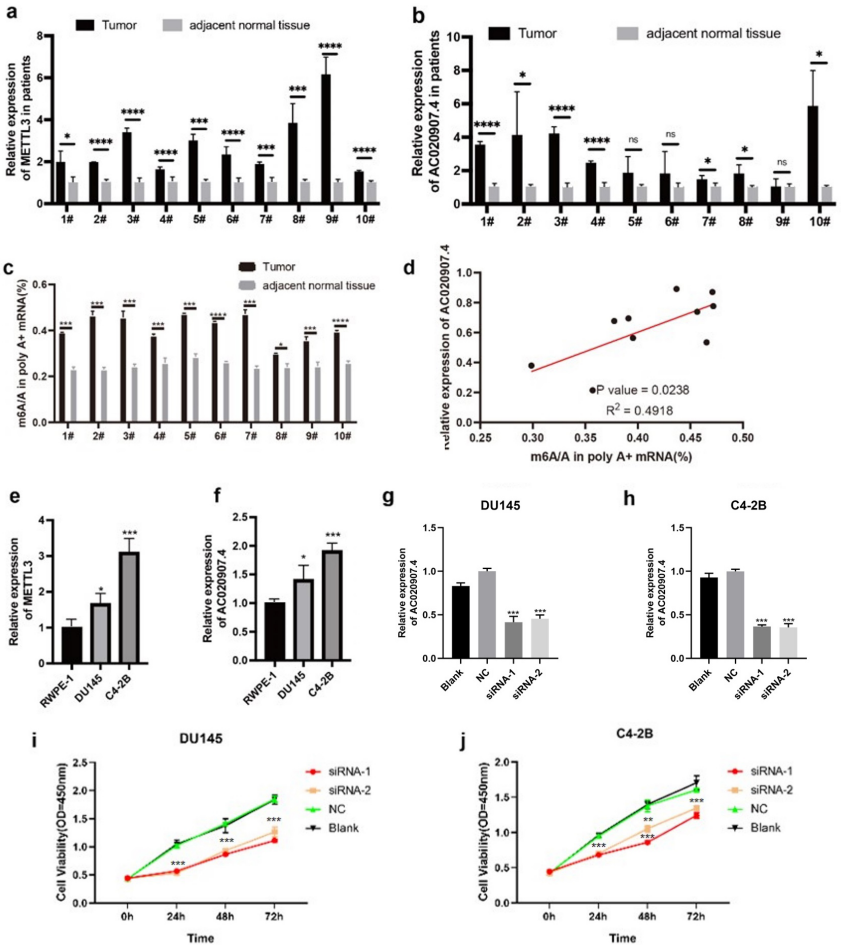

Fig. 5. Experimental validation of one selected long non-coding RNA, AC020907.4, in tissue samples and cell lines. (a) Expression of methyltransferase 3 (*METTL3*) in prostate cancer (PC) tissue samples and paired healthy tissue, error bars: mean ± Standard deviation (SD); n = 3 replicates; two-tailed Student's *t*-test was used for statistical analysis. (b) Expression of AC020907.4 in PC tissue samples and paired healthy tissue, error bars: mean ± SD; n = 3 replicates; two-tailed Student's *t*-test was used for statistical analysis. (c) Relative m6A level in PC tissue samples and paired healthy tissue, error bars: mean ± SD; n = 3 replicates; two-tailed Student's *t*-test was used for statistical analysis. (d) Correlation analysis between relative m6A level and AC020907.4 in PC tissue samples. (e) Expression of METTL3 in RWPE-1, DU145 and C4-2B, error bars: mean ± SD; n = 3 replicates; one-way ANOVA was used for statistical analysis. (f) Expression of AC020907.4 in RWPE-1, DU145 and C4-2B, error bars: mean ± SD; n = 3 replicates; one-way ANOVA was used for statistical analysis. (g) Downregulation of AC020907.4 in the siRNA-1 and siRNA-2 groups in the DU145 cell line, error bars: mean ± SD; n = 3 replicates; one-way ANOVA was used for statistical analysis, reference group: negative control (NC) group. (h) Downregulation of AC020907.4 in the siRNA-1 and siRNA-2 groups in the C4-2B cell line, error bars: mean ± SD; n = 3 replicates; one-way ANOVA was used for statistical analysis, reference group: NC group. (i) Growth curves for DU145 after transfection with siRNAs or the NC and blank group by the cell counting kit-8 (CCK-8) assay, error bars: mean ± SD; n = 3 replicates; two-way ANOVA was used for statistical analysis, reference group: NC group. (j) Growth curves for C4-2B after transfection with siRNAs or the NC and blank group by the CCK-8 assay. *, $p < 0.05$; **, $p < 0.01$; ***, $p < 0.001$; ****, $p < 0.0001$; ns, no significance. Error bars: mean ± SD; n = 3 replicates; two-way ANOVA was used for statistical analysis, reference group: NC group. ANOVA, analysis of variance; siRNA, small interfering RNA.

particular, the model improves the predictive power for the prognosis of T3–4 patients ($p < 0.001$) (Fig. 8e,f), which can serve as a reference for the precise medication and treatment protocol required. Consistent with previous findings, high-risk patients tend to have poor outcomes in several clinical subgroups.

Differentially Expressed mRNAs in the Low-Risk and High-Risk Groups

We used R software to identify the differentially expressed genes in the low-risk and high-risk groups. In total, 155 mRNAs were classified as differentially expressed in these two groups (**Supplementary Fig. 2a**).

Journal of
BIOLOGICAL REGULATORS
and Homeostatic Agents

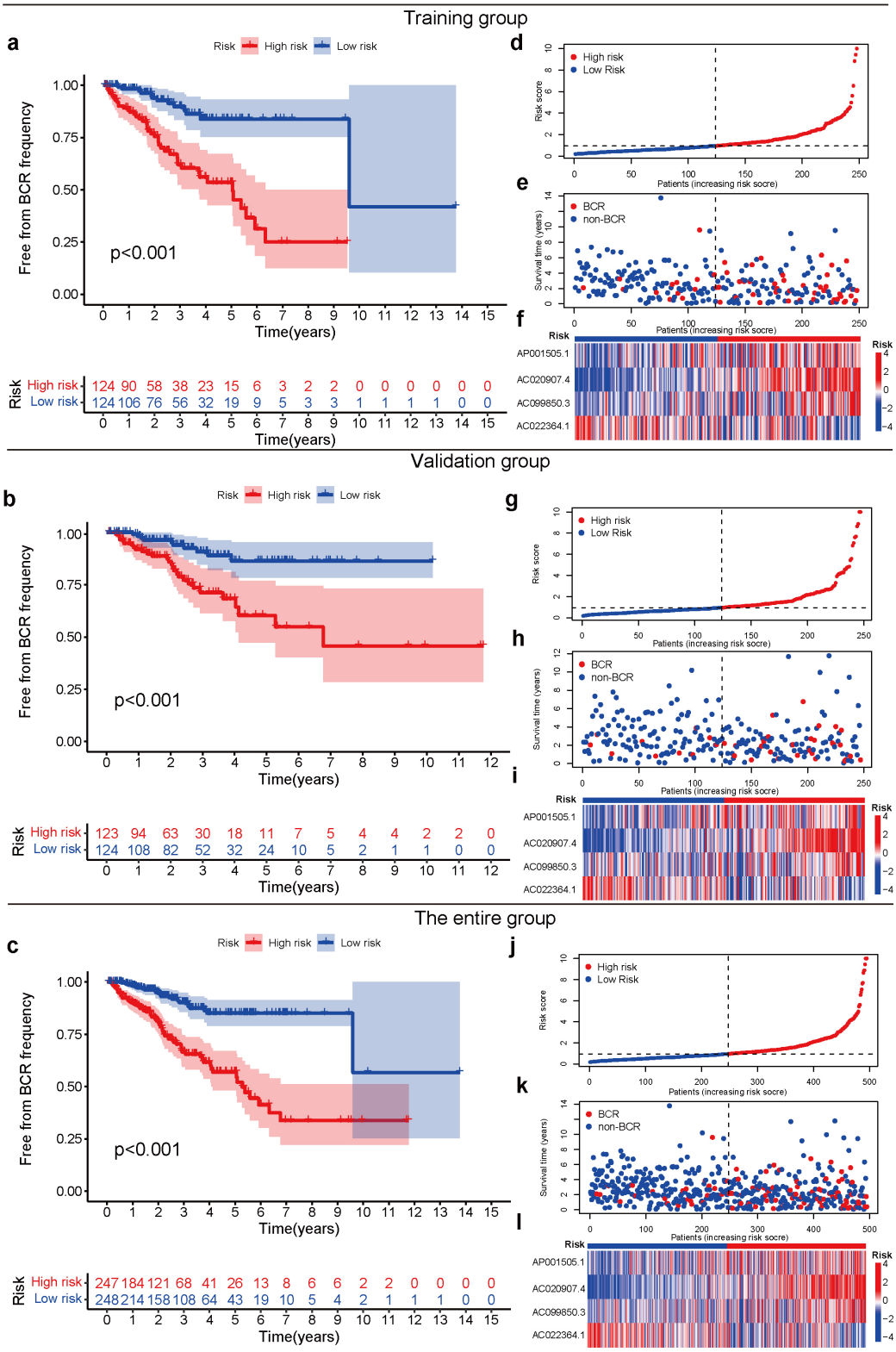

Fig. 6. Biochemical recurrence (BCR) in the different groups. (a) Kaplan–Meier plot for the low-risk and high-risk patients in the training group. (b) Kaplan–Meier plot for the low-risk and high-risk patients in the validation group. (c) Kaplan–Meier plot for the low-risk and high-risk patients in the entire group. (d) Different risk scores in the training group. (e) BCR distribution of patients in the training group. (f) Number of selected long non-coding RNAs (lncRNAs) in the training group. (g) Different risk scores in the validation group. (h) BCR distribution plot for patients in the validation group. (i) Expression of the selected lncRNAs in the validation group. (j) Different risk scores in the entire group. (k) BCR distribution plot for patients in the entire group. (l) Expression of selected lncRNAs in the entire group.

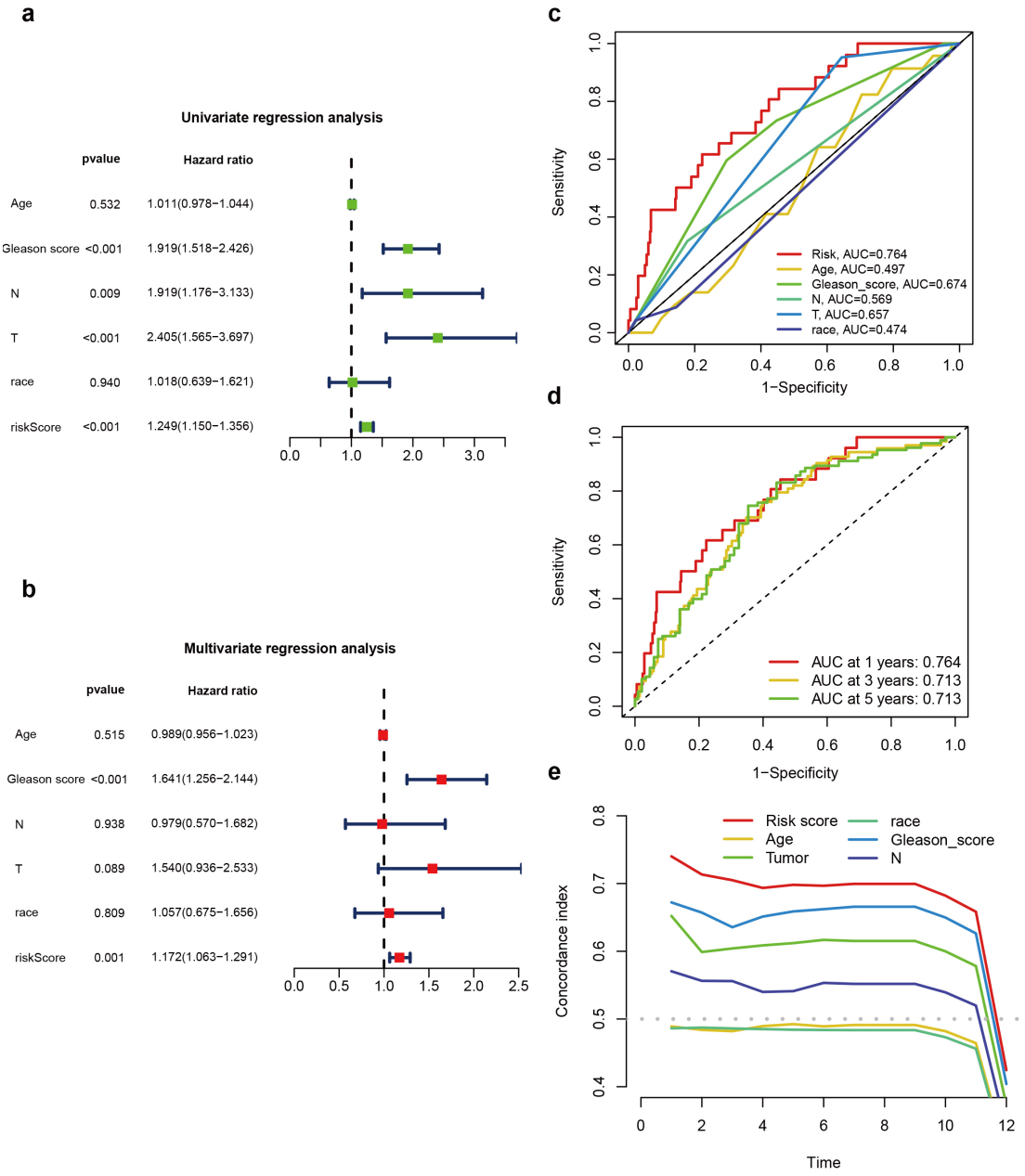

Fig. 7. Independence evaluation of the m6A-related long non-coding RNA model from other clinical information. Receiver operating characteristic (ROC) and concordance index (C-index) curves were utilised to assess the model's effectiveness. (a) Forest plot of the univariate Cox regression analysis. (b) Forest plot of the multivariate Cox regression analysis. (c) Risk scores and clinical information were assessed through the ROC curve using the entire group. The area under the curve (AUC) for the risk score = 0.764, and the cutoff value is 0.615 ($p < 0.05$). (d) Risk score in the training group was calculated using a time-dependent ROC curve. The AUCs are 0.764, 0.713 and 0.713 at 1-year, 3-year and 5-year survival points, and the cutoff value is 0.628, 0.784 and 0.781, respectively ($p < 0.05$). (e) The clinical information and risk scores were investigated using the C-index.

In addition, the GO pathway analysis suggested that these genes were strongly enriched in several molecular functions and biological processes related to cancer pathogenesis (**Supplementary Fig. 2b**). Detailed information on the differentially expressed genes from the GO analyses is shown in (**Supplementary Fig. 2b**).

Discussion

Prostate cancer is a highly complex and heterogeneous tumour, and castration is usually the treatment of choice. However, after a median of 18–24 months of hormone therapy, almost all patients progress to castration-resistant PC (CRPC); unfortunately, there are currently no effective

Journal of
BIOLOGICAL REGULATORS
and Homeostatic Agents

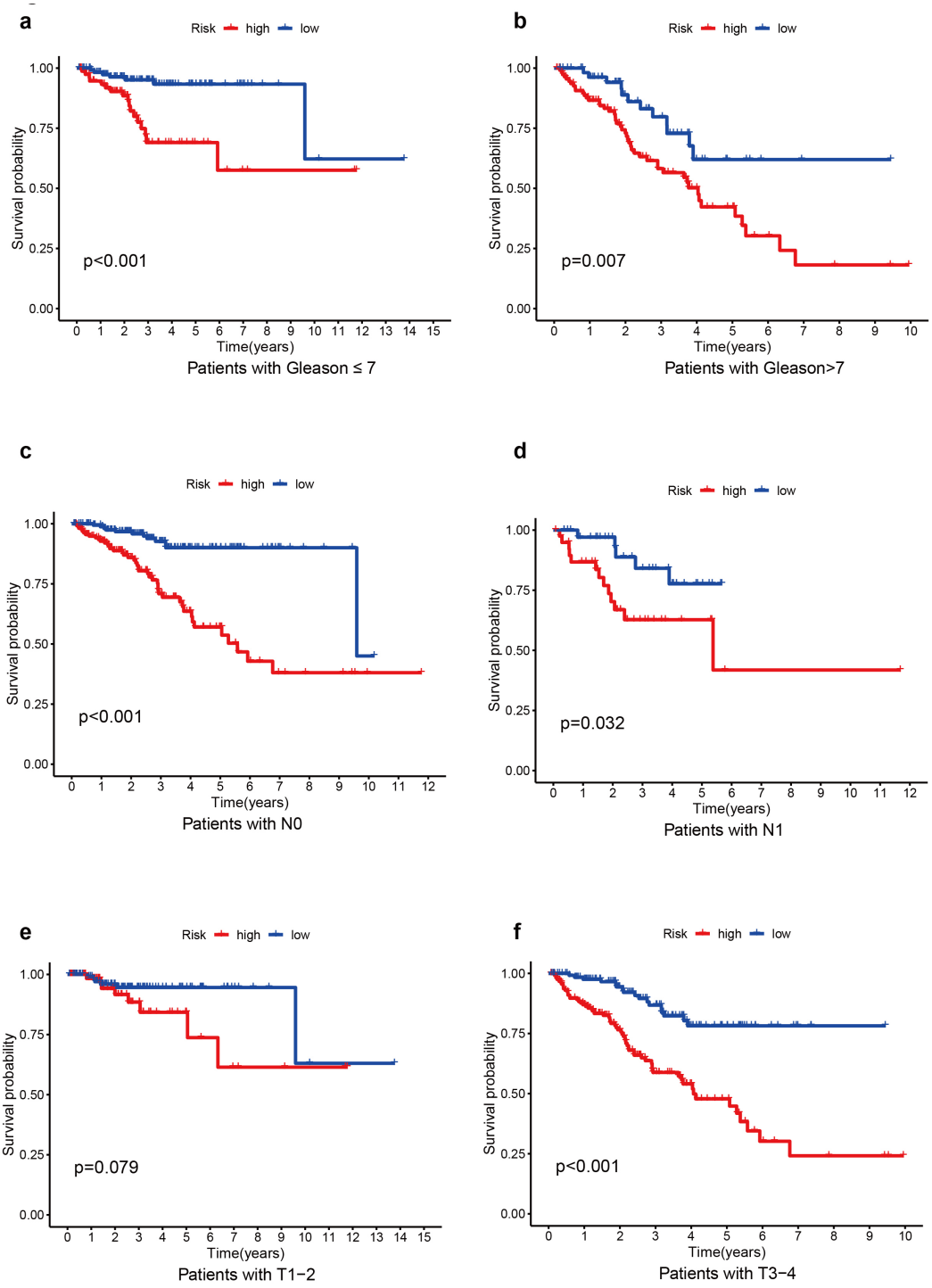

Fig. 8. Interaction between clinical information and risk scores investigated using a Kaplan–Meier plot. (a) Kaplan–Meier plot of low-risk and high-risk patients with Gleason scores ≤7. (b) Kaplan–Meier plot of low-risk and high-risk patients with Gleason scores >7. (c) Kaplan–Meier plot of low-risk and high-risk patients in the N0 group. (d) Kaplan–Meier plot of low-risk and high-risk patients in the N1 group. (e) Kaplan–Meier plot of low-risk and high-risk patients in the T1–2 group. (f) Kaplan–Meier plot of low-risk and high-risk patients in the T3–4 group.

treatments for CRPC [1]. Although plenty of therapies have been applied to improve the prognosis, drug resistance can still occur in patients with advanced hormone-refractory PC and CRPC [5]. Therefore, investigating the mechanisms at the molecular level and distinguishing reliable and accurate biomarkers are needed for the diagnosis, prevention and development of novel treatments.

The modification of m6A RNA is indispensable in post-transcriptional regulation and has been found in different types of ncRNAs, including lncRNAs, tRNAs, microRNAs and mRNAs [8]. Numerous studies have claimed that m6A-related lncRNAs may affect tumours from various perspectives [7,14,17]. For example, m6A modulators affect the m6A modification of lncRNAs, which affects the structure of the lncRNAs and enhances their stability. As a result, m6A modifications of lncRNAs can influence tumour development to some extent. Research is needed to determine the detailed interaction between lncRNAs and m6A modification in PC to identify new biomarkers for early clinical treatment and the prediction of disease progression.

In this study, we established a model of four m6A-related lncRNAs to predict BCR in patients with PC by analysing TCGA (n = 499) and CPGEA (n = 208) datasets. Patients with PC were divided into two subtypes that exhibited different outcomes. This study also verified the expression and function of AC020907.4, one of the four selected m6A-related lncRNAs, in PC tissue samples and cell lines. This study may help clinicians identify patients with a high BCR risk and develop personalised treatment plans for these patients. In addition, this study may help researchers understand the detailed molecular mechanism of PC pathogenesis.

The model identified four lncRNAs: AC020907.4, AC022364.1, AC099850.3 and AP001505.1. Of these, AC022364.1 and AP001505.1 were newly identified biomarkers for PC, having not been previously reported, whereas AC020907.4 and AC099850.3 are known in several types of tumours as prognostic biomarkers. For example, a high level of AC020907.4 was found in clear cell renal cell carcinoma, and it can be utilised for the prediction of OS in these patients [37]. In this study, patients with a high level of AC020907.4 had a poor prognostic indication. The expression of AC099850.3 was also found to be upregulated in non-small cell lung cancer tissue samples and was verified as a biomarker for this disease [38]. Moreover, both AC020907.4 and AC099850.3 were found to be associated with the autophagy process of cancer; AC020907.4 is active in the autophagy of clear cell renal cell carcinoma [38], and AC099850.3 is related to autophagy in hepatocellular carcinoma [39]. Plenty of studies have demonstrated that m6A modification is strongly correlated with autophagy in cancer [40, 41]. Alpha-ketoglutarate-dependent dioxygenase (FTO), an m6A demethylase, can inhibit autophagy and maintain the accumulation of FTO [42]. Moreover, YTHDF1, an m6A reader, is related to hypoxia-induced autophagy and the progression of autophagy-associated hepatocellular carcinoma [43]. We hypothesise that AC020907.4 and AC099850.3 may interfere with the autophagy of PC through m6A modification. Further research is essential to verify this hypothesis.

This study has some limitations. We used TCGA and the CPGEA databases to identify the m6A-related lncRNAs; however, we were unable to identify the detailed mechanism underlying these lncRNAs and m6A modification. We did verify the model in the entire group, but a larger sample size of patients with PC from different medical centres is required for further validation. The expression of lncRNAs was detected in the tumour tissue as a biomarker for predicting PC prognosis, but it may be more practical to detect this expression in the urine or blood of patients.

Conclusions

This study systematically identified m6A-related lncRNAs in PC, constructed a model for the prediction of BCR in patients with PC and validated the model's stability and effectiveness. The model was used independently as a marker for predicting BCR in our study and can provide novel insights for treating PC.

Availability of Data and Materials

All data generated or analyzed during this study are included in this published article.

Author Contributions

YFW, QZL and LYY contributed to the concept and designed the research study. YFW and XZ performed the research. QWY and XMZ provided materials for experimental design, participated in discussing plans and acquired data. WGC contributed to the analysis and interpretation of the data. All authors contributed to editorial changes in the manuscript. All authors read and approved the final manuscript. All authors have participated sufficiently in the work to take public responsibility for appropriate portions of the content and agreed to be accountable for all aspects of the work in ensuring that questions related to its accuracy or integrity.

Ethics Approval and Consent to Participate

This study was conducted in accordance with the Declaration of Helsinki and approved by the Ethics Committee of Kunshan Hospital of Traditional Chinese Medicine. All participants signed an informed consent form for inclusion in the study. The ethical approval number for this study was KZY2020-09.

Acknowledgment

We thank TopEdit (https://www.topeditsci.com) for its supports preparing this manuscript.

Journal of
BIOLOGICAL REGULATORS
and Homeostatic Agents

Funding

The research was funded by the Kunshan Research and development project (No. KSZ2203). The research was funded by the Special Scientific Research Fund of Suzhou Science and Technology Bureau (No. SYSD2019226).

Conflict of Interest

The authors declare no conflict of interest.

Supplementary Material

Supplementary material associated with this article can be found, in the online version, at https://doi.org/10.23812/j.biol.regul.homeost.agents.20243806.390.

References

[1] Siegel RL, Miller KD, Fuchs HE, Jemal A. Cancer Statistics, 2021. CA: A Cancer Journal for Clinicians. 2021; 71: 7–33.

[2] Sung H, Ferlay J, Siegel RL, Laversanne M, Soerjomataram I, Jemal A, *et al*. Global Cancer Statistics 2020: GLOBOCAN Estimates of Incidence and Mortality Worldwide for 36 Cancers in 185 Countries. CA: A Cancer Journal for Clinicians. 2021; 71: 209–249.

[3] Daskivich TJ, Howard LE, Amling CL, Aronson WJ, Cooperberg MR, Kane CJ, *et al*. Competing Risks of Mortality among Men with Biochemical Recurrence after Radical Prostatectomy. The Journal of Urology. 2020; 204: 511–517.

[4] Pak S, You D, Jeong IG, Kim YS, Hong JH, Kim CS, *et al*. Time to biochemical relapse after radical prostatectomy and efficacy of salvage radiotherapy in patients with prostate cancer. International Journal of Clinical Oncology. 2019; 24: 1238–1246.

[5] Cornford P, Bellmunt J, Bolla M, Briers E, De Santis M, Gross T, *et al*. EAU-ESTRO-SIOG Guidelines on Prostate Cancer. Part II: Treatment of Relapsing, Metastatic, and Castration-Resistant Prostate Cancer. European Urology. 2017; 71: 630–642.

[6] Van den Broeck T, van den Bergh RCN, Arfi N, Gross T, Moris L, Briers E, *et al*. Prognostic Value of Biochemical Recurrence Following Treatment with Curative Intent for Prostate Cancer: A Systematic Review. European Urology. 2019; 75: 967–987.

[7] Wang J, Lin H, Zhou M, Xiang Q, Deng Y, Luo L, *et al*. The m6A methylation regulator-based signature for predicting the prognosis of prostate cancer. Future Oncology. 2020; 16: 2421–2432.

[8] Huang H, Weng H, Chen J. m^6A Modification in Coding and Non-coding RNAs: Roles and Therapeutic Implications in Cancer. Cancer Cell. 2020; 37: 270–288.

[9] Zhong X, Yu J, Frazier K, Weng X, Li Y, Cham CM, *et al*. Circadian Clock Regulation of Hepatic Lipid Metabolism by Modulation of m^6A mRNA Methylation. Cell Reports. 2018; 25: 1816–1828.e4.

[10] Tu B, Song K, Zhou Y, Sun H, Liu ZY, Lin LC, *et al*. METTL3 boosts mitochondrial fission and induces cardiac fibrosis by enhancing LncRNA GAS5 methylation. Pharmacological Research. 2023; 194: 106840.

[11] Yang L, Tian S, Zheng X, Zhang M, Zhou X, Shang Y, *et al*. N6-methyladenosine RNA methylation in liver diseases: from mechanism to treatment. Journal of Gastroenterology. 2023; 58: 718–733.

[12] Nicastro G, Abis G, Klein P, Esteban-Serna S, Gallagher C, Chaves-Arquero B, *et al*. Direct m6A recognition by IMP1 underlays an alternative model of target selection for non-canonical methyl-readers. Nucleic Acids Research. 2023; 51: 8774–8786.

[13] Benak D, Kolar F, Zhang L, Devaux Y, Hlavackova M. RNA modification m^6Am: the role in cardiac biology. Epigenetics. 2023; 18: 2218771.

[14] Liu L, Li L, Zu W, Jing J, Liu G, Sun T, *et al*. PIWI-interacting RNA-17458 is oncogenic and a potential therapeutic target in cervical cancer. Journal of Cancer. 2023; 14: 1648–1659.

[15] Zhang Q, Luan J, Song L, Wei X, Xia J, Song N. Malignant Evaluation and Clinical Prognostic Values of M6A RNA Methylation Regulators in Prostate Cancer. Journal of Cancer. 2021; 12: 3575–3586.

[16] Li C, Zhang K, Gong Y, Wu Q, Zhang Y, Dong Y, *et al*. Based on cuproptosis-related lncRNAs, a novel prognostic signature for colon adenocarcinoma prognosis, immunotherapy, and chemotherapy response. Frontiers in Pharmacology. 2023; 14: 1200054.

[17] Roy L, Chatterjee O, Bose D, Roy A, Chatterjee S. Noncoding RNA as an influential epigenetic modulator with promising roles in cancer therapeutics. Drug Discovery Today. 2023; 28: 103690.

[18] Cai C, Shu K, Chen W, Ding J, Guo Z, Wei Y, *et al*. Construction and validation of a model based on immunogenic cell death-associated lncRNAs to predict prognosis and direct therapy for kidney renal clear cell carcinoma. Aging. 2023; 15: 5304–5338.

[19] Mitobe Y, Takayama KI, Horie-Inoue K, Inoue S. Prostate cancer-associated lncRNAs. Cancer Letters. 2018; 418: 159–166.

[20] Jiang M, Cheng Y, Wang D, Lu Y, Gu S, Wang C, *et al*. Transcriptional network modulated by the prognostic signature transcription factors and their long noncoding RNA partners in primary prostate cancer. eBioMedicine. 2021; 63: 103150.

[21] Zheng ZQ, Li ZX, Zhou GQ, Lin L, Zhang LL, Lv JW, *et al*. Long Noncoding RNA FAM225A Promotes Nasopharyngeal Carcinoma Tumorigenesis and Metastasis by Acting as ceRNA to Sponge miR-590-3p/miR-1275 and Upregulate ITGB3. Cancer Research. 2019; 79: 4612–4626.

[22] Luo P, Li S, Long X. N6-methyladenosine RNA modification in PD-1/PD-L1: Novel implications for immunotherapy. Biochimica et Biophysica Acta. Reviews on Cancer. 2023; 1878: 188873.

[23] Liu W, Zhang Z, Luo X, Qian K, Huang B, Deng J, *et al*. M6A Promotes Colorectal Cancer Progression via Regulating the miR-27a-3p/BTG2 Pathway. Journal of Oncology. 2023; 2023: 7097909.

[24] Ni W, Yao S, Zhou Y, Liu Y, Huang P, Zhou A, *et al*. Long noncoding RNA GAS5 inhibits progression of colorectal cancer by interacting with and triggering YAP phosphorylation and degradation and is negatively regulated by the m^6A reader YTHDF3. Molecular Cancer. 2019; 18: 143.

[25] Lang C, Yin C, Lin K, Li Y, Yang Q, Wu Z, *et al*. m^6 A modification of lncRNA PCAT6 promotes bone metastasis in prostate cancer through IGF2BP2-mediated IGF1R mRNA stabilization. Clinical and Translational Medicine. 2021; 11: e426.

[26] Weinstein JN, Collisson EA, Mills GB, Shaw KRM, Ozenberger BA, Ellrott K, *et al*. The Cancer Genome Atlas Pan-Cancer analysis project. Nature Genetics. 2013; 45: 1113–1120.

[27] Li J, Xu C, Lee HJ, Ren S, Zi X, Zhang Z, *et al*. A genomic and epigenomic atlas of prostate cancer in Asian populations. Nature. 2020; 580: 93–99.

[28] Gu C, Shi X, Qiu W, Huang Z, Yu Y, Shen F, *et al*. Comprehensive Analysis of the Prognostic Role and Mutational Characteristics of m6A-Related Genes in Lung Squamous Cell Carcinoma. Frontiers in Cell and Developmental Biology. 2021; 9: 661792.

[29] Robinson MD, McCarthy DJ, Smyth GK. edgeR: a Bioconductor package for differential expression analysis of digital gene expression data. Bioinformatics. 2010; 26: 139–140.

[30] Ito K, Murphy D. Application of ggplot2 to Pharmacometric Graphics. CPT: Pharmacometrics & Systems Pharmacology. 2013; 2: e79.
[31] Tibshirani R. The lasso method for variable selection in the Cox model. Statistics in Medicine. 1997; 16: 385–395.
[32] Tang Z, Wu Y, Sun D, Xue X, Qin L. A novel prognostic immunoscore based on The Cancer Genome Atlas to predict overall survival in colorectal cancer patients. Bioscience Reports. 2021; 41: BSR20210039.
[33] Kamarudin AN, Cox T, Kolamunnage-Dona R. Time-dependent ROC curve analysis in medical research: current methods and applications. BMC Medical Research Methodology. 2017; 17: 53.
[34] Van Oirbeek R, Lesaffre E. An application of Harrell's C-index to PH frailty models. Statistics in Medicine. 2010; 29: 3160–3171.
[35] Yu G, Wang LG, Han Y, He QY. clusterProfiler: an R package for comparing biological themes among gene clusters. Omics. 2012; 16: 284–287.
[36] Uhlén M, Björling E, Agaton C, Szigyarto CAK, Amini B, Andersen E, *et al*. A human protein atlas for normal and cancer tissues based on antibody proteomics. Molecular & Cellular Proteomics. 2005; 4: 1920–1932.
[37] Li X, Yu H, Wei Z, Gou X, Liang S, Liu F. A Novel Prognostic Model Based on Autophagy-Related Long Non-Coding RNAs for Clear Cell Renal Cell Carcinoma. Frontiers in Oncology. 2021; 11: 711736.
[38] Zhou J, Zhang M, Dong H, Wang M, Cheng Y, Wang S, *et al*. Comprehensive Analysis of Acetylation-Related lncRNAs and Identified AC099850.3 as Prognostic Biomarker in Non-Small Cell Lung Cancer. Journal of Oncology. 2021; 2021: 4405697.
[39] Jia Y, Chen Y, Liu J. Prognosis-Predictive Signature and Nomogram Based on Autophagy-Related Long Non-coding RNAs for Hepatocellular Carcinoma. Frontiers in Genetics. 2020; 11: 608668.
[40] Huang L, Shao J, Xu X, Hong W, Yu W, Zheng S, *et al*. WTAP regulates autophagy in colon cancer cells by inhibiting FLNA through N6-methyladenosine. Cell Adhesion & Migration. 2023; 17: 1–13.
[41] Jo H, Shim K, Jeoung D. Roles of RNA Methylations in Cancer Progression, Autophagy, and Anticancer Drug Resistance. International Journal of Molecular Sciences. 2023; 24: 4225.
[42] Cui YH, Yang S, Wei J, Shea CR, Zhong W, Wang F, *et al*. Autophagy of the m^6A mRNA demethylase FTO is impaired by low-level arsenic exposure to promote tumorigenesis. Nature Communications. 2021; 12: 2183.
[43] Li Q, Ni Y, Zhang L, Jiang R, Xu J, Yang H, *et al*. HIF-1α-induced expression of m6A reader YTHDF1 drives hypoxia-induced autophagy and malignancy of hepatocellular carcinoma by promoting ATG2A and ATG14 translation. Signal Transduction and Targeted Therapy. 2021; 6: 76.